Cryoenzymic Studies on Myosin Subfragment 1: Perturbation of an Enzyme Reaction by Temperature and Solvent†

J. A. Biosca,‡ F. Travers, D. Hillaire,§ and T. E. Barman*

ABSTRACT: The effects of temperature and solvent on myosin subfragment 1 ATPase have been studied. Under all of the conditions used the data could be fitted to the Bagshaw–Trentham pathway:

$$M + ATP \overset{K_1}{\rightleftharpoons} M\cdot ATP \overset{k_{+2}}{\underset{k_{-2}}{\rightleftharpoons}} M^*\cdot ATP \overset{k_{+3}}{\underset{k_{-3}}{\rightleftharpoons}} M^{**}\cdot ADP\cdot P_i \overset{k_{+4}}{\underset{k_{-4}}{\rightleftharpoons}} M^*\cdot ADP\cdot P_i \overset{k_{+5}}{\underset{k_{-5}}{\rightleftharpoons}} M^*\cdot ADP \overset{k_{+6}}{\underset{k_{-6}}{\rightleftharpoons}} M\cdot ADP \overset{K_7}{\rightleftharpoons} M + ADP$$

Ethylene glycol (40%) was used as the cryosolvent; this makes K_1 and k_{+2} measurable and allows for temperature studies over an extensive temperature range (+35 to −20 °C) and thus to reasonably accurate thermodynamic parameters. The following techniques were used: ATP chase (for K_1 and k_{+2}); P_i burst (k_{+2} or $k_{+3} + k_{-3}$); single-turnover P_i burst [$k_0 = k_{+4}K_3/(1 + K_3)$] absorption stopped flow (k_{+2} or $k_{+3} + k_{-3}$); steady state (k_{+6} or k_0). Myosin provides examples of causes for nonlinear Arrhenius and van't Hoff plots. A temperature-induced structural change is exemplified by a "jump" in an Arrhenius plot of k_{+2} and "breaks" in van't Hoff plots of K_1 and K_3. A change in rate-limiting step is illustrated from stopped-flow experiments ($k_{obsd} \sim k_{+2}$ at low and $\sim k_{+3} + k_{-3}$ at high temperatures) and steady-state experiments ($k_{cat} \sim k_{+6}$ at low and $\sim k_0$ at high temperatures). A third cause is illustrated by k_0: an Arrhenius plot of k_0 is nonlinear since there is a break in K_3. These studies illustrate the use of temperature perturbation as a way of revealing reaction intermediates and of defining the conditions required for the isolation of a particular intermediate. Thus, at −15 °C K_3 and k_{+4} are small and a key intermediate, M*·ATP, accumulates with a half-life of 12 mn. Unlike the preceding steps, step 4 (k_{+4}) is little affected by the solvent (ethylene glycol, KCl) or by the temperature-induced structural change of myosin, and its $\Delta H^{\ddagger}$ is low. The modulations of this step may be restricted to a specific interaction of M**·ADP·P_i with actin.

Muscle contraction consists of the cyclic attachment and detachment of myosin heads to actin filaments. The energy needed for these processes is supplied by the hydrolysis of ATP[1] by the myosin heads. A detailed knowledge of myosin ATPase is, therefore, a prerequisite for an understanding of muscle contraction and its mechanism has received much attention (Trentham et al., 1976; Taylor, 1979; Adelstein & Eisenberg, 1980). These studies have led to a seven-step mechanism (see Scheme I), the Bagshaw–Trentham pathway (e.g., Bagshaw et al., 1974), where M represents myosin or one of its proteolytic fragments (subfragment 1 or heavy meromyosin) and where different protein conformations are indicated by asterisks. Equilibrium constants are expressed as $K_i = k_{+i}/k_{-i}$.

Scheme I

$$M + ATP \overset{K_1}{\rightleftharpoons} M\cdot ATP \overset{k_{+2}}{\underset{k_{-2}}{\rightleftharpoons}} M^*\cdot ATP \overset{k_{+3}}{\underset{k_{-3}}{\rightleftharpoons}} M^{**}\cdot ADP\cdot P_i \overset{k_{+4}}{\underset{k_{-4}}{\rightleftharpoons}} M^*\cdot ADP\cdot P_i \overset{k_{+5}}{\underset{k_{-5}}{\rightleftharpoons}} M^*\cdot ADP \overset{k_{+6}}{\underset{k_{-6}}{\rightleftharpoons}} M\cdot ADP \overset{K_7}{\rightleftharpoons} M + ADP$$

Actin interacts with certain of the intermediates of this pathway and this modifies the rate constants concerned. Lymn & Taylor (1971) have proposed a scheme relating the actomyosin pathway to muscle contraction; this has recently been expanded and a summary is provided by Goldman et al. (1982).

There remain several important questions. In particular, at which step is the bulk of the chemical energy of ATP converted to the mechanical energy required for the relative sliding of the myosin and actin filaments? The model of Huxley [for example, Huxley (1969)] predicts that this energy transduction is in some way associated with the movements of the myosin cross bridges. Thus, most authors agree that the question can be narrowed down to one asking about the conformational changes of the intermediates of the actomyosin system during the course of ATP hydrolysis.

Because of the rapidity of certain of the key steps, the myosin and, in particular, the actomyosin ATPases are difficult to study. A way of overcoming this problem is to lower the temperature, and by use of organic solvents as antifreezes subzero conditions can be attained (Douzou, 1977).

A cryoenzymic study on the overall myosin ATPase reaction has been carried out with ethylene glycol as the antifreeze (Bêchet et al., 1979; Travers & Hillaire, 1979). Recently, the temperature dependency of the binding of ATP in the range +35 to −15 °C was studied; in an Arrhenius plot of k_{+2} there was a "jump" at 10–15 °C, which was interpreted as being caused by a phase change (Biosca et al., 1983). As this work proceeded, it became clear that the effects on the system of ethylene glycol and temperature could not always be distinguished from those produced by other physicochemical parameters such as pH or ionic strength. In order to clarify the situation, we study here the effects of ethylene glycol, ionic strength, pH, and, in particular, the temperature on the first four steps of myosin subfragment 1 ATPase (Scheme I). For temperature-dependency studies to be useful, the data must be extensive and the system was investigated over a wide temperature range: 35 to −20 °C.

Four methods were used. Three involve the flow quench technique: ATP chase experiments (which determine K_1 and

† From INSERM U 128, CNRS, B.P. 5051, 34033 Montpellier Cedex, France. *Received August 29, 1983.*

‡ Permanent address: Department of Biochemistry, Facultat de Ciencies, Universitat Autonoma de Barcelona, Barcelona, Spain. J.A.B. received a short-term fellowship from FEBS.

§ Present address: Centre de Recherche de Biochimie Macromoléculaire, CNRS, B.P. 5051, 34033 Montpellier Cedex, France.

[1] Abbreviations: ATP, adenosine 5′-triphosphate; ADP, adenosine 5′-diphosphate; P_i, inorganic orthophosphate; AMP-PNP, adenylyl imidodiphosphate; SF-1, myosin subfragment 1.

0006-2960/84/0423-1947$01.50/0

Table I: Variation of Certain of the Kinetic Constants of SF-1 ATPase with Experimental Conditions at 15 °C

experimental conditions[a]			kinetic constants[b]						
ethylene glycol [% (v/v)]	KCl (mM)	pH	K_1 (M^{-1})	k_{+2} (s^{-1})	$k_{+3} + k_{-3}$ (s^{-1})	K_3	k_{+4} (s^{-1})	k_{+6} (s^{-1})	k_{cat} (s^{-1})
40	5	8	1.25×10^5	16	22 (±3)	1	0.12	0.2	0.06
40	150	8	9×10^3	45	21 (±3)	2	0.09		0.06
40	150	6.4	3.7×10^4	8	>>8	2.1	0.06		0.04
40	150	9				1.4	0.12		0.07
0	1	8				2.3	0.12		0.08
0	5	8	$<5 \times 10^3$	>160	19	2.2	0.12		0.08
0	25	8				2.7	0.10		0.07
0	150	8			90[c]				0.08

[a] For full details, see the legend to Figure 1. [b] Values for K_1, k_{+2}, and $k_{+3} + k_{-3}$ (recalculated, see the text) are from Barman et al. (1983). k_{+4} was calculated from K_3 and k_0 (single-turnover experiments) and k_{+6} extrapolated (Figure 8). Where indicated, means ± SD are given for $k_{+3} + k_{-3}$ obtained by computer simulation and eq 1. [c] Present work.

k_2); P_i burst experiments (k_2 or $k_3 + k_{-3}$, depending on the experimental conditions); single-turnover experiments (K_3 and k_{+4}; Bagshaw & Trentham, 1973). The fourth, stopped flow, is less specific and can give information on k_2 or $k_{+3} + k_{-3}$ [e.g., Chock et al. (1979)].

A further aim of the present work was to exploit the temperature as a perturbant of a reaction pathway, and for this purpose the SF-1 ATPase system served as an example. First, certain causes for nonlinear Arrhenius plots are analyzed. Second, it is shown how the temperature can apparently modify the SF-1 ATPase pathway by shifting a temperature-sensitive equilibrium. This illustrates the usefulness of temperature perturbation in the study of enzyme mechanisms.

Materials and Methods

Proteins and Reagents. Myosin and its subfragment 1 were prepared from rabbit skeletal muscle (Weeds & Taylor, 1975). The isoenzymes of SF-1 were given by Dr. R. Kassab. These had been prepared and purified as described by Weeds & Taylor (1975).

SF-1 concentrations were estimated at 280 nm by assuming $A^{1\%}_{1cm} = 7.5$ (Wagner & Weeds, 1977). Molar concentrations were expressed in terms of an M_r of 110000 (Margossian & Lowey, 1978). SF-1 active site concentrations were determined from ATP chase experiments (Barman et al., 1983). [γ-^{32}P]ATP was obtained from Amersham (International Amersham, Bucks, U.K.).

Quenched-Flow Experiments. The quench-flow apparatus used have already been described (Barman et al., 1980). One is a rapid flow quench apparatus, taking samples from 4 to 280 ms, and the other a time delay flow quench apparatus (0.4 s upward). Both are thermostatically controlled to ±0.2 °C. Three types of experiments were carried out [also, see Barman et al. (1983)]. In ATP chase experiments, SF-1 plus [γ-^{32}P]ATP reaction mixtures were quenched in a large molar excess (>300) of unlabeled ATP. The quenched reaction mixtures were incubated at 25 °C and after 2 min stopped by the addition of an equal volume of 5.4% (w/v) trichloroacetic acid containing 1 mM NaH_2PO_4, and the [^{32}P]P_i was determined by the method of Reimann & Umfleet (1978).

In P_i burst and single-turnover experiments reaction mixtures were quenched directly in trichloroacetic acid and the [^{32}P]P_i was determined.

The experimental conditions used for the individual experiments are indicated in the figure legends.

Stopped-Flow Experiments. These were carried out by using a stopped-flow apparatus mounted on an Aminco DW 2 spectrophotometer set to the dual function and thermostatically controlled to ±0.2 °C. The increase in the optical density of SF-1–ATP reaction mixtures was followed at 290 nm; the procedure used has already been described (Travers & Barman, 1980).

Slow Reaction Experiments. ATP chase experiments at less than −10 °C and all steady-state experiments were carried out in thermostatically controlled beakers as described by Travers & Hillaire (1979).

Treatment of Kinetic Data. The data were interpreted with reference to Scheme I.

An analysis of cold ATP chase experiments has already been given (Barman et al., 1983, and references cited therein). In brief, the kinetics of these give

$$k = k_{+2}\frac{K_1[ATP]_0}{1 + K_1[ATP]_0}$$

assuming $k_{-2} \ll k_{cat} \ll k$ and $[M]_0 \ll [ATP]_0$. $[M]_0$ is the SF-1 active site concentration.

In P_i burst experiments the formation of M**·ADP·P_i + P_i is followed; the kinetics obtained depend on the ratio k:(k_{+3} + k_{-3}), which is sensitive to the experimental conditions (Barman et al., 1983). Here the phosphate determined is given by

$$\frac{[P_i]_{tot}}{[M]_0} = \frac{B}{k - (k_{+3} + k_{-3})}[-(k_{+3} + k_{-3})(1 - e^{-kt}) + k(1 - e^{-(k_{+3}+k_{-3})t})] \quad (1)$$

with the same assumptions as for ATP chase experiments. Estimates of $k_{+3} + k_{-3}$ were obtained by an improvement of a previous procedure (Barman et al., 1983). Thus, k was obtained from ATP chase experiments and B is the value of the experimentally obtained amplitude of the P_i burst. With these values, the experimental points were fitted by adjustment to a series of values of $k_{+3} + k_{-3}$ by using the KINFIT program of Knack & Röhm (1981) and an Apple II 48K computer. Under conditions where $k \sim k_{+3} + k_{-3}$ a lag phase is obtained and the error in $k_{+3} + k_{-3}$ is relatively large (for example, Figure 1 and Table I).

In single-turnover experiments ($[M]_0 > [ATP]_0$) the formation of P_i is followed on the time scale $t \simeq 1/k_4$. In this time range, K_3 describes a rapid equilibrium and as shown by Bagshaw & Trentham (1973)

$$\frac{[P_i]_{tot}}{[ATP]_0} = 1 - \frac{1}{1 + K_3}e^{-k_0 t} \quad (2)$$

where $[P_i]_{tot} = [M^{**}\cdot ADP\cdot P_i] + [P_i]$ at time t, $[ATP]_0$ = total ATP, and $k_0 = k_4K_3/(1 + K_3)$. The terms of this equation are illustrated in Figure 2.

Steady-state experiments lead to k_{cat}. This is a complex function of the individual rate constants of Scheme I, but when

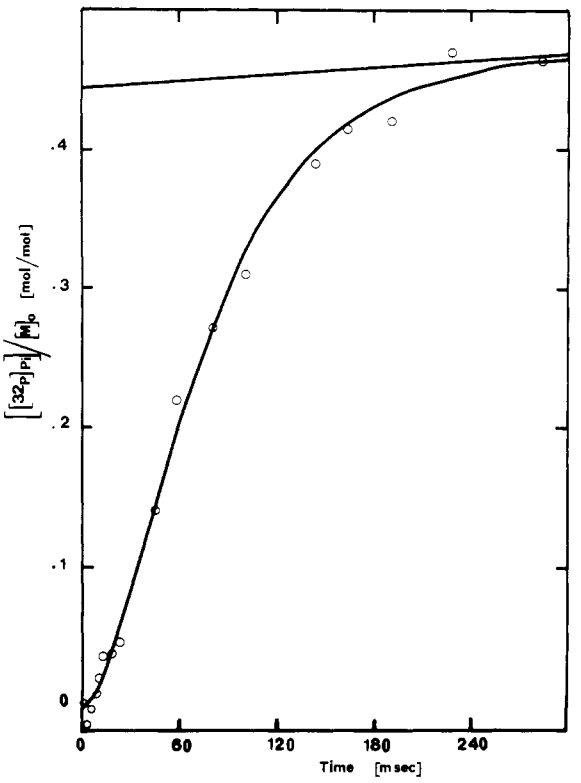

FIGURE 1: Time course for P_i burst in 5 mM KCl and 40% ethylene glycol at 25 °C. The reaction mixture was 5 μM SF-1 and 50 μM [γ-^{32}P]ATP. The buffer was 50 mM Tris base, 5 mM KCl, 2 mM magnesium acetate, 0.1 mM dithiothreitol, and 40% ethylene glycol adjusted to pH 8.0 with acetic acid. The continous curve was computer simulated by using eq 1 with k = 22.5 s^{-1} and B = 0.44 and gave $k_{+3} + k_{-3}$ = 27.9 (±2.6) s^{-1}. For other details, see the text.

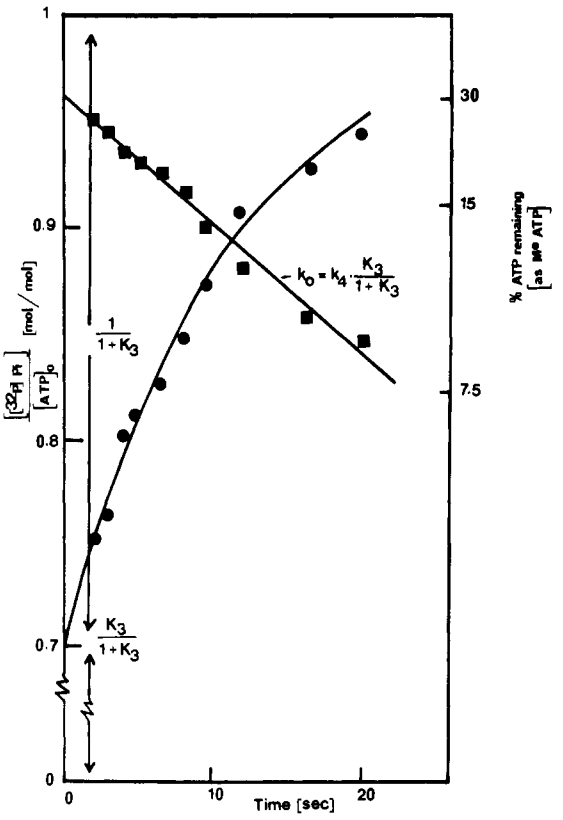

FIGURE 2: Single-turnover experiment in 1 mM KCl and H_2O at 15 °C. The reaction mixture was 6 μM SF-1 active sites and 2 μM [γ-^{32}P]ATP. The buffer was 50 mM Tris base, 1 mM KCl, 2 mM magnesium acetate, and 0.1 mM dithiothreitol adjusted to pH 8 with acetic acid. The first-order plot gave k_{cat} = 0.08 s^{-1} and the extrapolation to t = 0 gave K_3 = 2.3. The figure illustrates the terms of eq 2.

the assumptions that steps 1, 5, and 7 are rapid equilibria and that $k_{+4} \ll k_{+3} + k_{-3}$ under all of the conditions used here are made, a simplified expression is

$$\frac{1}{k_{cat}} = \frac{1}{k_{+2}} + \frac{1 + K_3}{K_3}\frac{1}{k_{+4}} + \frac{1}{k_{+6}} \quad (3)$$

Results

ATP Chase Experiments. These lead directly to values for K_1 and k_{+2}; their variation with experimental conditions has been determined (Biosca et al., 1983; Barman et al., 1983). The temperature dependency of k_2 (−15 to +35 °C) in 40% ethylene glycol and 5 mM KCl is given in Figure 3.

ATP chase experiments were carried out on the separated isoenzymes of SF-1 and the results obtained are given in Figure 4. These were carried out under conditions where $[ATP]_0 > 1/K_1$ for the mixed population (Biosca et al., 1983) and k_2 = 0.032 (±0.006) s^{-1} for SF-1 (A-1) and 0.023 (±0.004) s^{-1} for SF-1 (A-2). This closeness in values is in agreement with, for example, the conclusions of Taylor & Weeds (1977) and Sivaramakrishnan & Burke (1982), namely, that the ATPase activities of the SF-1 isoenzymes are very similar, if not identical. The experiments carried out below were carried out on the mixed population.

P_i Burst Experiments. The temperature dependency of $k_{+3} + k_{-3}$ in the temperature range 5–35 °C and in 40% ethylene glycol and 5 mM KCl is shown in Figure 3. It was not possible to determine the temperature dependency of $k_{+3} + k_{-3}$ below 12 °C. Here, the kinetics of ATP chase and P_i burst experiments were identical, which shows that k_{+2} is smaller than $k_{+3} + k_{-3}$ (i.e., that k_{+2} is rate limiting). In the higher temperature range (>12 °C) there were transient lag phases in P_i burst experiments (e.g., Figure 1); here $k_{+3} + k_{-3} \sim k_{+2}$ and computer simulation was used to obtain $k_{+3} + k_{-3}$ (also see Table I).

Stopped-Flow Experiments. When ATP interacts with myosin, certain tryptophan residues are perturbed, which give rise to an increase in absorption at 290 nm and a fluorescence enhancement. Most of the pre-steady-state kinetics on myosin have been carried out by using fluorescence stopped flow (Bagshaw et al., 1974; Johnson & Taylor, 1978; Chock et al., 1979), but there are difficulties in assigning the optical signal. Thus, certain workers maintain that it is primarily due to M*·ATP, others to M**·ADP·P_i, and yet others to both [for a discussion, see Chock et al. (1979) and Geeves & Trentham (1982)]. However, the kinetics obtained are first order [but see Johnson & Taylor (1978)] and very close to the P_i burst kinetics under the same conditions [e.g., Chock et al. (1979)].

Here, the interaction of ATP with SF-1 was followed by absorption stopped flow. The Arrhenius plot of the rate constant obtained was determined in 40% ethylene glycol and high KCl (0.15 M); this was not linear and is illustrated in Figure 5. The amplitude decreased as the temperature decreased, which could, at least in part, be due to a decrease in the M**·ADP·P_i to M*·ATP ratio, i.e., a decrease in K_3 (see below). The Arrhenius plots (5–35 °C) for the absorption stopped-flow and P_i burst kinetics under various conditions are given in Figure 6.

Single-Turnover Experiments. A typical experiment is given in Figure 2; this method leads directly to k_0 and K_3 and thus k_{+4}.

The temperature dependencies of K_3, k_0, and the derived k_{+4} are given in Figure 7. Below +5 °C, K_3 decreased sharply

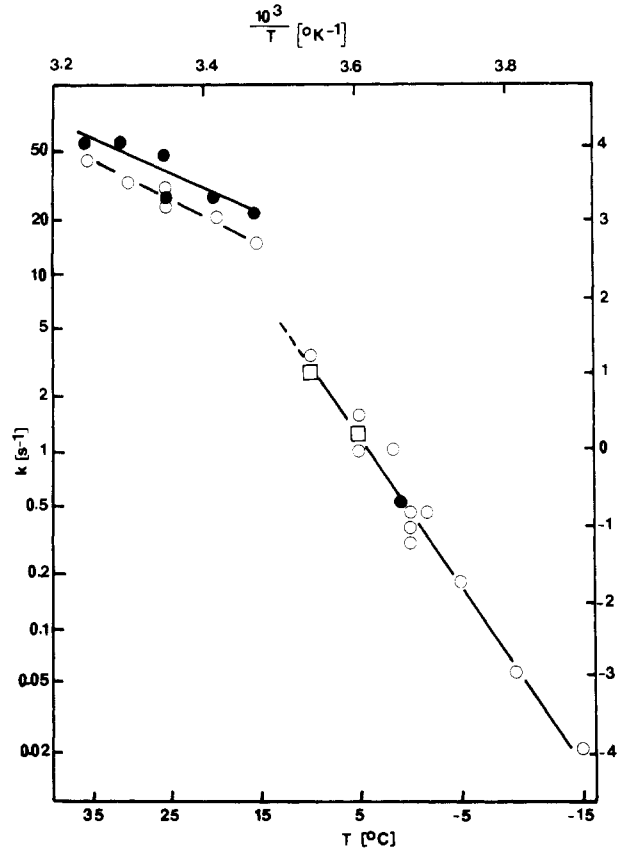

FIGURE 3: Arrhenius plots of the rate constants obtained from ATP chase, P_i burst, and stopped-flow experiments in 5 mM KCl and 40% ethylene glycol. The experiments are indicated as ATP chase (○), P_i burst (●), and stopped flow (□). For further details, see the legend to Figure 1 and the text. The ATP chase data are from Biosca et al. (1983).

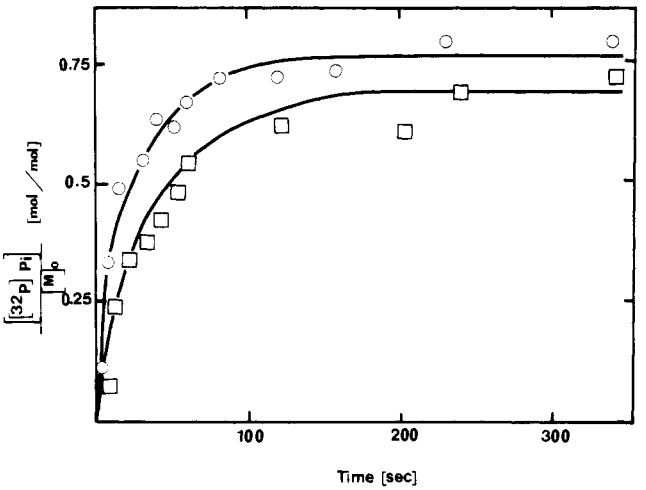

FIGURE 4: Time courses for the binding of ATP to the SF-1 isoenzymes at −15 °C. The reaction mixtures contained 1 μM SF-1 (A1) (○) or SF-1 (A2) (□) and 5 μM [γ-^{32}P]ATP. The buffer used is indicated in the legend to Figure 1 except that the pH was 7.5. From the curves k_{+2} = 0.032 (±0.006) s^{-1} for SF-1 (A1) and 0.023 (±0.004) s^{-1} for SF-1 (A2). In this figure $[M]_0$ refers to the protein concentration.

with a decrease in temperature; this decreases the accuracy of the experiment and single-turnover experiments were limited to −5 °C.

A van't Hoff plot of K_3 could be fitted to two lines with a break in the 10–15 °C region. This break occurs in the same temperature region as for the jump in k_{+2} (Biosca et al., 1983). The values calculated for k_{+4} on either side of the critical 10–15 °C region were treated separately according to the

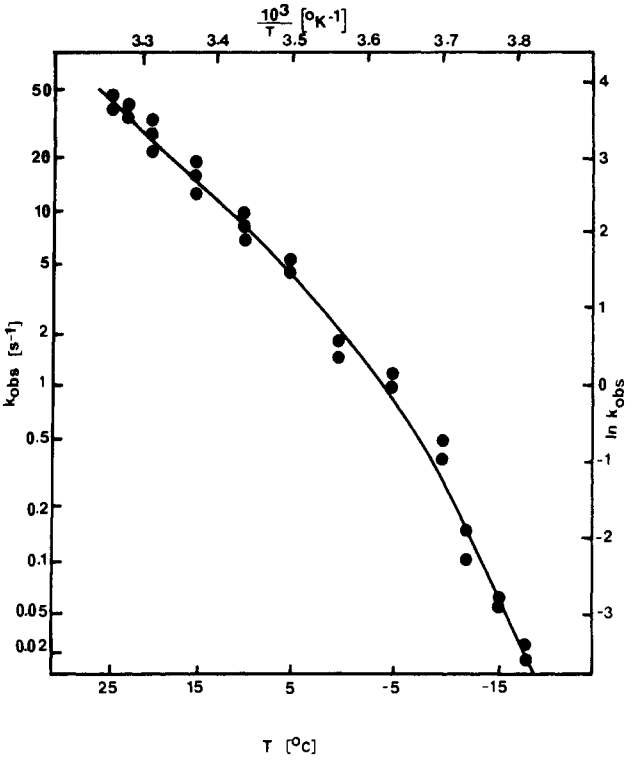

FIGURE 5: Arrhenius plot of the rate constants obtained from stopped-flow experiments in 0.15 M KCl and 40% ethylene glycol. The reaction mixtures were 10 μM SF-1 and 0.5 mM ATP. The buffer used is indicated in the legend to Figure 1 except that KCl = 0.15 M. For other details, see the text.

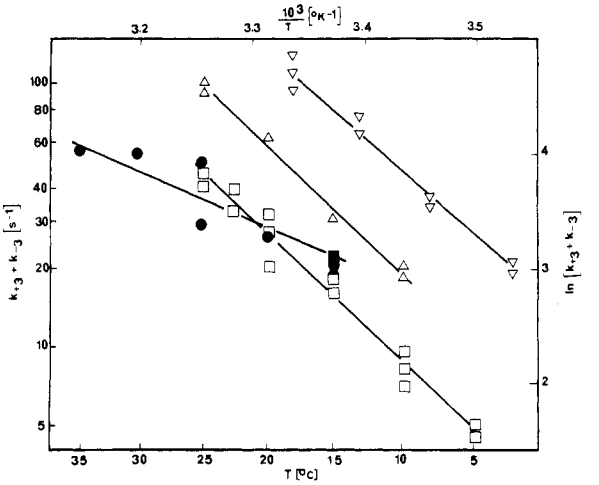

FIGURE 6: Arrhenius plots of the rate constants obtained from P_i burst and stopped-flow experiments under different experimental conditions. These were 5 mM KCl and 40% ethylene glycol [P_i burst (●)], 0.15 M KCl and 40% ethylene glycol [P_i burst (■); stopped flow (□)], 5 mM KCl [stopped flow (△)], and 0.15 M KCl [stopped flow (▽)]. For further details, see the legend to Figure 1 and the text.

Arrhenius relationship, and the two lines obtained practically coincide (Figure 7). It appears, therefore, that k_{+4} is little affected by the 12 °C phase transition.

From the computer-simulated temperature dependencies of K_3 and k_{+4} (Figure 7), the temperature dependency of k_0 was calculated by using $k_0 = k_{+4}K_3/(1 + K_3)$. As shown in Figure 7 the fit agrees well with the experimental points.

Steady-State Experiments. Previous work (Travers & Hillaire, 1979) showed that an Arrhenius plot of k_{cat} was nonlinear. This is presumably due to a change in rate-limiting step: k_0 in the high temperature range and k_{+6} in the low temperature range (Malik & Martonosi, 1972; Schaub &

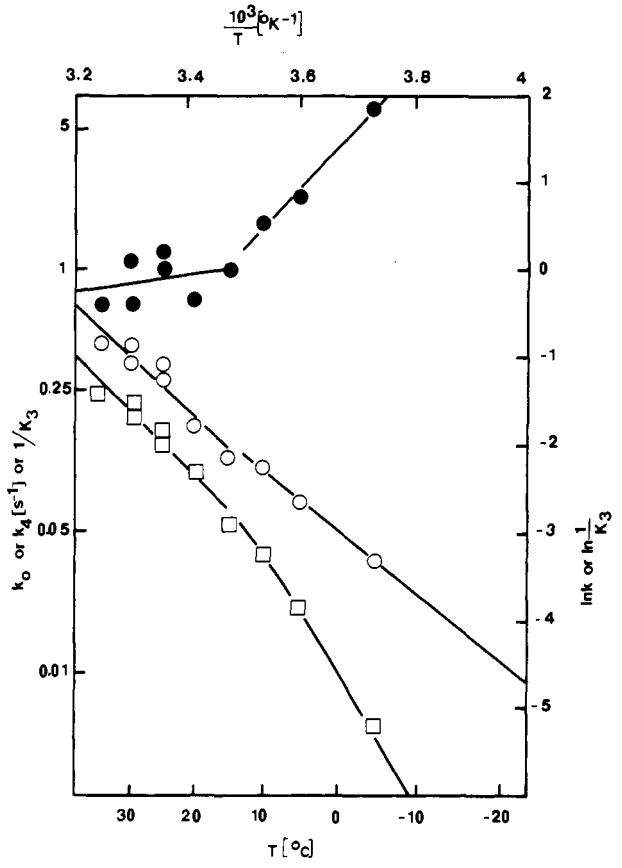

FIGURE 7: Temperature dependencies of K_3, k_{+4}, and k_0 in 5 mM KCl and 40% ethylene glycol. $1/K_3$ (●) and k_0 (□) are from single-turnover experiments and k_{+4} (○) was calculated from $k_4 = k_0(1 + K_3)/K_3$. The curves are computer fitted, with the data above and below the phase transition (at 12 °C) being treated separately. For other details, see the legends to Figures 1 and 2.

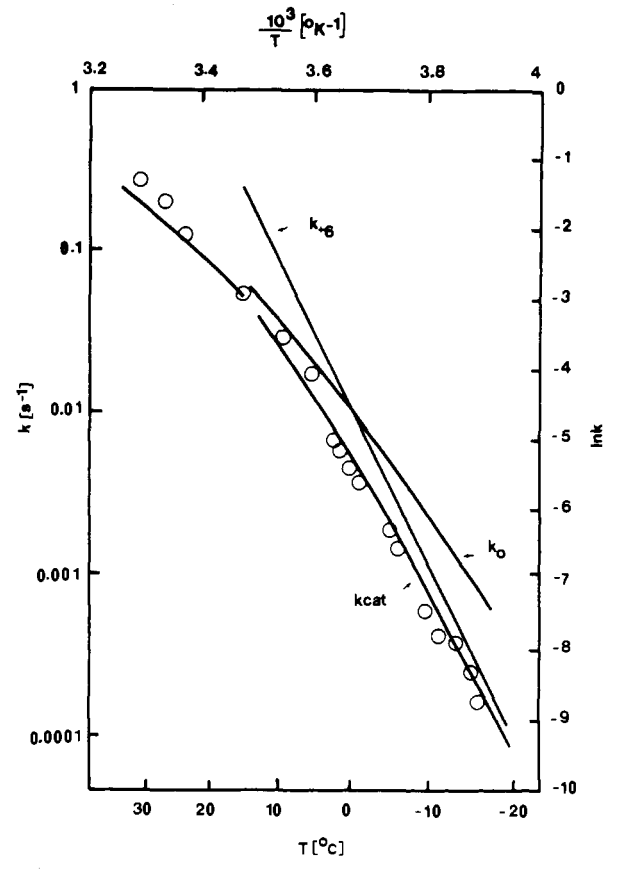

FIGURE 8: Arrhenius plots of k_{cat}, k_0, and k_{+6} in 5 mM KCl and 40% ethylene glycol. The curves are computer simulated with k_{cat} from steady-state experiments and k_0 from Figure 7; k_{+6} was adjusted to $1/k_{cat} = 1/k_{+2} + 1/k_0 + 1/k_{+6}$. The buffer used is indicated in the legend to Figure 1.

Watterson, 1973; Bagshaw & Trentham, 1974).

This experiment was repeated under the present experimental conditions, and the result obtained is illustrated in Figure 8. As before, the plot was nonlinear. An Arrhenius plot for k_{+6} was derived from eq 3, i.e., $1/k_{+6} = 1/k_{cat} - 1/k_{+2} - 1/k_0$ and is also given in Figure 8.

From the computer-simulated temperature dependencies of k_{+2} (Figure 3), k_{+4} and K_3 (Figure 7), and k_{+6} (Figure 8), the temperature dependency of k_{cat} was calculated by using eq 3. As shown in Figure 8, the fit agrees well with the experimental points.

Effect of Solvent Composition on Certain of the Kinetic Constants of Scheme I. The results are summarized in Table I. K_1 and k_{+2} are rather sensitive to 40% ethylene glycol and KCl (Barman et al., 1983). In water $k_{+3} + k_{-3}$ is sensitive to KCl: when the KCl concentration increases from 5 to 150 mM, it increases about 4.5-fold. This is in agreement with Geeves & Trentham (1982). The effect of 40% ethylene glycol depends on the concentration of KCl; at 5 mM KCl it has little effect whereas at 150 mM KCl it decreases $k_{+3} + k_{-3}$ about 4.5-fold. These results, however, must be qualified by the possibility that $k_{+3} + k_{-3}$ is affected by the SF-1 phase transition [which appears to be sensitive to ethylene glycol and KCl (Biosca et al., 1983)] rather than to the solvent composition itself.

The constants K_3 and k_{+4} are relatively insensitive to the composition of the solvent. It is noteworthy that k_{+4} is unaffected by 40% ethylene glycol. The effects of changes in KCl concentration or pH on K_3 and k_0 are in agreement with previous findings (Taylor, 1979).

Thermodynamic Parameters for Certain of the Kinetic Constants of SF-1 ATPase. These were obtained from the various temperature-dependency studies and are summarized in Table II.

The thermodynamic parameters pertaining to K_1 and k_{+2} have been discussed (Biosca et al., 1983). At above 0 °C, in 0.15 M KCl and 40% ethylene glycol or water (Table II), the $\Delta H^{\ddagger}$ of $k_{+3} + k_{-3}$ was 75 (±9) kJ mol^{-1}. This compares with previous work in water, pH 8, and 0.1 M KCl: Sleep et al. (1981), from experiments at 3, 10, and 20 °C, give 94 kJ mol^{-1}, Chock et al. (1979) obtained $k_{+3} + k_{-3}$ at 5, 10, 15, and 20 °C and from their values a $\Delta H^{\ddagger}$ of about 110 kJ mol^{-1} can be calculated. Both groups obtained their results from stopped-flow experiments. In agreement with Taylor (1979), Bêchet et al. (1979), and Kodama (1981), K_3 decreases as the temperature decreases. The $\Delta H^{\ddagger}$ for k_{+6} is 134 kJ mol^{-1}; Hillaire & Travers (1979) obtained 120 kJ mol^{-1}. Bagshaw & Trentham (1974) and Kodama (1981) estimated 130 kJ mol^{-1}, Sleep et al. (1981) 100 kJ mol^{-1}, and Bêchet et al. (1979) 116 kJ mol^{-1}.

Discussion

Titration of Myosin ATPase Sites. An important feature of the Bagshaw–Trentham Scheme (Scheme I) is that it assumes that the myosin heads are kinetically identical and, in particular, that both bind ATP irreversibly. This allows for ATP chase experiments and thus the titration of all ATPase sites of myosin itself or of the separated heads (SF-1).

In the present work a large number of ATP chase experiments were carried out, and the results are statistically significant. In particular, the titration values obtained were

Table II: Certain Thermodynamic Parameters for SF-1 ATPase in 40% Ethylene Glycol and 5 mM KCl[a]

constant	temp (°C)	value	ΔH° or $\Delta H^\ddagger$ (kJ mol^{-1})	ΔG° or $\Delta G^\ddagger$ (kJ mol^{-1})	ΔS° or $\Delta S^\ddagger$ (J mol^{-1} K^{-1})
K_1	0	3 (±0.4) × 10^5 M^{-1}	46 (±8)	29	62 (±30)
	25	1 (±0.2) × 10^5 M^{-1}	21 (±6)	29	−27 (±20)
k_{+2}	0	0.35 (±0.05) s^{-1}	119 (±10)	69	184 (±40)
	25	30 (±3) s^{-1}	40 (±3)	64	−88 (±10)
$k_{+3} + k_{-3}$	25	36 (±5) s^{-1}	34 (±8)	64	−100 (±25)
$k_{+3} + k_{-3}$[b]	25	45 (±6) s^{-1}	75 (±9)	63	40 (±30)
K_3	0	0.25 (±0.04)	58 (±7)	3	200 (±40)
	25	1.1 (±0.1)	8.5 (±12)	0.3	25 (±70)
k_{+4}	0[c]	0.05 (±0.02) s^{-1}	39 (±2)	73	−124 (±8)
	25[d]	0.3 (±0.002) s^{-1}	44 (±6)	76	−107 (±20)
	mean[e]		40 (±2)		
k_{+6}[f]	0	0.01 s^{-1}	134	77	210
	25	1.7 s^{-1}[g]			

[a] Except where otherwise stated, conditions as in the legend to Figure 1. [b] In 0.15 M KCl; the $\Delta H^\ddagger$ values obtained in water were very similar (Figure 6). [c] <10 °C. [d] >15 °C. [e] Entire range (Figure 7). [f] Values are extrapolated from Figure 8. [g] Trentham et al. (1976) obtained 1.4 s^{-1} at 21 °C and in water.

within the range 0.5–0.85 mol of active site/mol of SF-1 protein. We emphasize that the value obtained in a particular experiment depended on the SF-1 preparation used and not on the experimental conditions (ethylene glycol, pH, KCl, temperature). We are unable to determine the factor or factors responsible for this variation but it appears to be related to myosin itself rather than to the SF-1 prepared from it.

It is noteworthy that values less than 0.5 mol of active site/mol of SF-1 protein were rarely obtained. This may be significant—it could show that one myosin head is less stable than the other. This was not investigated further here. It could be an explanation for the suggestion of Tonomura [e.g., Tonomura & Inoue (1975)], namely, that whereas both myosin heads hydrolyze ATP, only one produces a P_i burst. According to this theory ATP is bound tightly to one head and weakly to the other head. However, as already discussed in detail by Chock & Eisenberg (1979) titration values greater than 0.5 (as found here) make this alternative ATPase pathway unlikely.

Causes of Nonlinear Arrhenius Plots. These have been discussed by several authors [e.g., Huennekens (1963), Kumamoto et al. (1971), Gutfreund (1972), Dixon & Webb (1979), and Londesborough (1980)]. Most published examples are of composite constants such as k_{cat} and there are few concerning the temperature dependencies of simple rate constants (Laidler & Peterman, 1979). Here a diagnosis of the effect of temperature on SF-1 ATPase provides examples of several of the causes for nonlinear Arrhenius plots. The full exploitation of such studies depends on an extensive temperature range, and the SF-1 ATP system was studied in the range −20 to +35 °C with 40% ethylene glycol as the cryosolvent.

The first cause for a nonlinear Arrhenius plot is that there is a temperature-induced conformational change in the enzyme or phase change. Such plots have sharp breaks or, rarely, jumps (Biosca et al., 1983). There are examples for the composite constant k_{cat} [e.g., Massey et al. (1966), Kumamoto et al. (1971), and Miyano (1983); membrane-bound enzymes are a special case, e.g., Parenti-Castelli et al. (1983)], and these have served as evidence for structural transitions at the break.

The evidence for a structural transition is more convincing when there is a break in the Arrhenius plot of a simple rate constant. With SF-1 there is a jump in the Arrhenius plot of k_{+2}, in the temperature region (10–15 °C) at which SF-1 aggregates. Most published work on SF-1 ATPase had presumably been carried out at temperatures below the structural transition [below 34 °C in water (Biosca et al., 1983)]. Under the same conditions as for the jump in k_{+2} (40% ethylene glycol, 5 mM KCl) there was a break in K_3 in the same temperature region, but because of the small variation it was difficult to discern a jump (Figure 7). Below the break, the ΔH° for K_3 was 58 kJ mol^{-1}. [Kodama & Woledge (1979) obtained 83 kJ mol^{-1}.] The $\Delta H^\ddagger$ for $k_{+3} + k_{-3}$ was obtained under various conditions and the differences found could be due to the structural transition. If so, it is 34 kJ mol^{-1} above and 75 kJ mol^{-1} below the transition (Figure 6 and Table II). It is thus very probable that there is a break in the Arrhenius plot of $k_{+3} + k_{-3}$, but as above the transition $k_3 + k_{-3} \sim k_{+2}$ and below $k_{+3} + k_{-3} > k_{+2}$ it was difficult to show this (Figure 3). It is noteworthy that k_{+4} is hardly affected by the phase transition (Figure 7).

Since ATP chase experiments were carried out under only one set of conditions [for an explanation, see Barman et al. (1983)], it is possible that the jump in the Arrhenius plot of k_{+2} is unrelated to the SF-1 aggregation: that the transition observed for both should be near 12 °C could be fortuitous. Thus, the thermodynamic characteristics of ADP and AMP-PNP binding to SF-1 have been studied in water and the $-\Delta H^\circ$/temperature curves had deflections at 13 °C. This was interpreted as being due to a structural transition (Kodama, 1981). Arrhenius plots of the ATPase activity of actomyosin and the walking rate of ants had sharp breaks at 16 °C (Levy et al., 1959). These temperatures compare with the critical 34–37 °C for the temperature-induced aggregation of SF-1 in water (Biosca et al., 1983). Nevertheless, the present studies strongly suggest that the Arrhenius and van't Hoff plot jumps and breaks are related to some temperature-induced structural transition, if not a structural aggregation, of SF-1.

The second class of nonlinear Arrhenius plot is purely kinetic in origin. Such plots are confined to composite rate constants, e.g., k_0 or k_{cat} (Figure 7 or 8, respectively). k_0 is a function of a rate constant (k_{+4}) and an equilibrium constant (K_3), and had both of these had linear temperature-dependency curves, an Arrhenius plot of k_0 would have been linear (at least in the temperature range available for enzyme studies). The nonlinearity of k_0 is a reflection of the break in the van't Hoff plot of K_3 (Figure 7); the Arrhenius plot of k_{+4} is probably linear. A similar situation presumably obtains with $k_{+3} + k_{-3}$; as K_3 varies with the temperature, the individual constants have different activation energies and there could be breaks in the Arrhenius plots of either or both. Because of the imprecision in $k_{+3} + k_{-3}$ this could not be experimentally confirmed.

When a composite rate constant is a function of two or more rate constants of very different energies of activation, the

contribution of each constant changes significantly as the temperature is changed. This is the classical "change in rate-limiting step" situation and is probably the most common cause of a nonlinear Arrhenius plot (Dixon & Webb, 1979). There are two possible examples on the SF-1 pathway.

First, the temperature dependency of k_{cat} is a function of k_0 (whose Arrhenius plot itself is nonlinear), k_{+2}, and k_{+6}. k_0 is rate limiting at high and k_{+6} at low temperatures [Figure 8; also see Travers & Hillaire (1979, and references cited therein)].

Second, the rate constants obtained from stopped-flow experiments are a function of k_2 and $k_{+3} + k_{-3}$, the relative contribution of which depends on the temperature (Figure 5). Now, at −15 °C (in 40% ethylene glycol and 0.15 M KCl) the kinetics of a stopped-flow experiment were first order and very similar to those obtained from ATP chase data obtained under the same conditions (result not shown), and they can therefore be assigned to k_{+2}. This situation also obtains in 5 mM KCl (Figure 3). At +15 °C, the stopped-flow kinetics are close to $k_{+3} + k_{-3}$ (P_i burst) but slower than k_{+2} (ATP chase, Table I) and here they can be assigned to $k_{+3} + k_{-3}$. However, in between these temperatures the situation is complex. Here k_{+2} and $k_{+3} + k_{-3}$ are presumably close and one would expect biphasic kinetic curves, but within the precision of the experiment none could be detected. An explanation for this is that both M*·ATP and M**·ADP·P_i (Scheme I) contribute toward the stopped-flow signal; this would hide any putative lag in M**·ADP·P_i formation (i.e., $k_{+3} + k_{-3}$). In this event, k_{obsd} can be expressed as a sum of two exponentials, and attempts were made to extract k_{+2} and $k_{+3} + k_{-3}$ from the data (i.e., by fitting kinetic curves to different amplitudes and rate constants) but without success. It is therefore difficult to assign the rate constants from stopped-flow experiments in the intermediate temperature range and to fully interpret Figure 3; nevertheless, the nonlinearity can largely be explained by a change in rate-limiting step: $k_{+3} + k_{-3}$ at high and k_{+2} at low temperatures.

A third cause of a nonlinear Arrhenius plot is that the solvent structure undergoes a structural transition. This was the explanation given for the kinetics of ribonuclease in water (Biosca et al., 1982). Here a break in an Arrhenius plot of k_{cat} was explained by a structural transition of water causing a conformational change. As the relevant physical constants for 40% ethylene glycol are unavailable, this possibility with SF-1 was not tested.

A problem inherent in temperature-dependency studies concerns the control of the pH or, more precisely, the temperature sensitivity of the pK of the buffer used. The temperature dependencies of the pK values of various buffers are given in detail by Douzou et al. (1976). The buffer used here (Tris) has a pH of 8 at 25 °C and 9.3 at −15 °C (the lowest temperature used). The question is, is there a pH effect superimposed on the Arrhenius effect in the various temperature-dependency studies? It does not help matters to adjust the pH of the buffer as the temperature is changed as this procedure overlooks the various enzyme groups whose pK values may also be temperature sensitive. Ideally one should determine the pH dependency of each kinetic step under each experimental condition (temperature, ethylene glycol, KCl, etc.).

We decided not to temperature correct the pH of the Tris buffer for two reasons. First, any amino acid residue(s) involved in the pH region in question (7.5–9) would be principally basic with pK values varying with the temperature as much as and in the same direction as Tris and there could, therefore, be a compensation effect. An example of this is given by arginine kinase (Travers et al., 1978). Here a pK concerned with k_{cat} (8 in 40% ethylene glycol at 20 °C) was studied as a function of the temperature. The buffer (Tris) was pH corrected as the temperature was varied. The ΔH for the pK of k_{cat} obtained (40 kJ) was close to the 46 kJ of Tris. Thus, had the pH of the Tris buffer not been corrected for the pK of the k_{cat} of arginine kinase would have been constant in the temperature range studied.

Second, in the pH range in question, several of the kinetic constants pertaining to SF-1 ATPase are relatively pH insensitive: K_3 (Table I), k_{+4} (Table I), and k_{+6} at −20 °C (Travers & Hillaire, 1979).

Possible Interpretation of the Sensitivities of the Kinetic Constants of SF-1 ATPase to the Experimental Conditions. Structural transitions are sensitive to the physicochemical properties of the medium, but it is difficult to rigorously interpret the thermodynamic parameters concerned. A solvent such as water is a reserve of thermal energy and has an important effect on these parameters. Attempts have been made to separate the various physicochemical properties of the solvent [for example, the viscosity (Beece et al., 1980) and the dielectric constant (Maurel, 1978)], but it remains difficult to quantify these effects. As a solvent, 40% ethylene glycol does not appear to greatly change the SF-1 structure. Limited tryptic digestion of SF-1 converts the heavy chain into three fragments (Mornet et al., 1979); 40% ethylene glycol affected neither the specificity nor the relative rate of the cleavage of the peptide bonds involved (J. A. Biosca, F. Travers, and T. E. Barman, unpublished experiments).

With SF-1 ATPase, k_{+2} and k_{+4} (both presumably involved in conformational changes) serve as extreme examples of the differences in sensitivities of rate constants to the experimental conditions. k_2 is very sensitive to the composition of the solvent (ethylene glycol, pH, KCl; Table I), to the structure of the environment (in 40% ethylene glycol and 5 mM KCl SF-1 aggregates above 10 °C), and to the temperature (high energy of activation below 10 °C). This suggests that there is a large solvent effect on k_{+2}. On the other hand, k_{+4} is much less sensitive to these perturbants (Table I); in particular, it is hardly affected by the structural transition (Figure 7) nor by 40% ethylene glycol. Step 3 (Scheme I) is intermediate in its sensitivity (Table I and Figures 3, 6, and 7). This step may involve a proton release and it has been suggested that K_3 should increase with pH (Chock, 1979). However, K_3 did not vary significantly with pH (Table I). This is in agreement with Bagshaw & Trentham (1974). It could be that the pK of the group involved in this proton release is outside the pH range studied or it could be ancillary to the kinetic processes governing step 3.

In summary, the first steps on the SF-1 pathway, which lead to the firm anchorage of ATP, are rather sensitive to the experimental conditions, but the chemical step and, in particular, the following isomerization are much less so. It is as though once the ATP is bound the system closes in upon itself and becomes isolated from the environment. This conclusion, deduced from kinetic data, is in agreement with certain structural data, namely, that the myosin active site has a "jaw"-like structure that closes up with the ATP bound (Wells & Yount, 1982, and references cited therein). The insensitivity of k_{+4} to nonspecific perturbants may be significant—its modulation may be restricted to a highly specific interaction of SF-1 with actin. This interaction is known to affect the SF-1 structure (Highsmith & Cook, 1983).

Apparent Modification of a Reaction Pathway by the Temperature. The effects of the temperature on the various k_{obsd} at SF-1 ATPase were complex but in each case explained as the result of normal thermodynamic processes. The data could be fitted to the Bagshaw–Trentham scheme over the large temperature range 35 to −15 °C [also see Bêchet et al. (1979)]. It is known that actin activates SF-1 over a similar temperature range (Trentham, 1977; Travers & Hillaire, 1979; Marston, 1982).

These studies illustrate the usefulness of the temperature as a perturbant in obtaining mechanistic information. For example, at −5 °C in 5 mM KCl and 40% ethylene glycol K_3 = 0.16 and the amplitude of a P_i burst experiment was small (0.14 mol of P_i/mol of active site). Lowering the temperature decreases the amplitude further. Under subzero conditions an SF-1 ATPase mechanism would therefore be (with the notation of Scheme I)

$$M + ATP \overset{K_1}{\rightleftharpoons} M{\cdot}ATP \xrightarrow{k_{+2}} M^*{\cdot}ATP \underset{P_i}{\overset{k_0}{\rightleftharpoons}} M^*{\cdot}ADP \xrightarrow{k_{+6}} M + ADP$$

When the temperature is increased, the P_i burst increases sharply and $M^{**}{\cdot}ADP{\cdot}P_i$ must be introduced as an intermediate. Further, although k_{+6} can be studied with ADP as ligand (Bagshaw & Trentham, 1974), cryoenzymology provides the conditions for its, albeit indirect, study with ATP [also see Bêchet et al. (1979) and Travers & Hillaire (1979)].

Another example of the temperature as a perturbant is the case of creatine kinase. At −15 or 4 °C, there were three phases of product (creatine phosphate) formation; this was attributed to enzyme–substrate and –product complexes (Travers et al., 1979; Barman et al., 1980). Above 20 °C there was no transient phase (Engelborghs et al., 1975; Travers et al., 1979).

In conclusion, temperature perturbation is one way of detecting "hidden" steps on a reaction pathway. But it is also a means of getting hold of intermediates for further study. A key intermediate on the SF-1 pathway is $M^*{\cdot}ATP$ (Geeves & Trentham, 1982), but because of a large K_3 and large k_0 it is difficult to study under ambient conditions. However, at −15 °C in 5 mM KCl K_3 and k_0 are small and $M^*{\cdot}ATP$ is a major intermediate with a half-life of about 12 min. Thus, one of the aims of cryoenzymology has been approached, namely, to provide the experimental conditons for the trapping of a reaction intermediate for structural studies such as by NMR (Douzou, 1977).

Interpretation of the Thermodynamic Parameters of SF-1 ATPase. Several authors warn against the overinterpretation of Arrhenius and, in particular, of van't Hoff plots [for example, Jencks (1969), Krug et al. (1976), Londesborough, (1980), and Keleti (1983)]. Here we calculated (Dixon & Webb, 1979) certain of the thermodynamic parameters pertaining to SF-1 ATPase (Table II), and we limit ourselves to very general comments. Where possible, the values are compared with those from previous work under Results.

The high $\Delta H^{\ddagger}$ values for k_{+2} and k_{+6} are noteworthy. Both involve protein isomerizations induced by nucleotide (Scheme I). As pointed out by Bagshaw & Trentham (1974), large activation energies can be associated with cooperative structural transitions of macromolecules. An alternative explanation would involve the solvent. The free energy for the chemical step (step 3, Scheme I) is close to zero. This is in common with a number of enzymes and has been used as a measure of enzyme efficiency [e.g., Wilkinson & Rose (1979) and Knowles (1980)]. The myosin case has been discussed by Gutfreund & Trentham (1975).

Acknowledgments

We thank Professor P. Douzou for support and encouragement. We are grateful to Dr. R. Kassab for supplies of the myosin SF-1 isoenzymes.

Registry No. ATP, 56-65-5; ATPase, 9000-83-3; KCl, 7447-40-7; ethylene glycol, 107-21-1.

References

Adelstein, R. S., & Eisenberg, E. (1980) *Annu. Rev. Biochem. 49*, 921–956.

Bagshaw, C. R., & Trentham, D. R. (1973) *Biochem. J. 133*, 323–328.

Bagshaw, C. R., & Trentham, D. R. (1974) *Biochem. J. 141*, 331–349.

Bagshaw, C. R., Eccleston, J. F., Eckstein, F., Goody, R. S., Gutfreund, H., & Trentham, D. R. (1974) *Biochem. J. 141*, 351–364.

Barman, T. E., Brun, A., & Travers, F. (1980) *Eur. J. Biochem. 110*, 397–404.

Barman, T. E., Hillaire, D., & Travers, F. (1983) *Biochem. J. 209*, 617–626.

Bêchet, J. J., Brêda, C., Guinand, S., Hill, M., & d'Albis, A. (1979) *Biochemistry 18*, 4080–4089.

Beece, D., Einsenstein, L., Frauenfelder, H., Good, D., Marden, M. C., Reinisch, L., Reynolds, A. H., Sorensen, L. B., & Yve, K. T. (1980) *Biochemistry 19*, 5147–5157.

Biosca, J. A., Travers, F., & Cuchillo, C. M. (1982) *Eur. J. Biochem. 124*, 151–156.

Biosca, J. A., Travers, F., & Barman, T. E. (1983) *FEBS Lett. 153*, 217–220.

Chock, S. P. (1979) *J. Biol. Chem. 254*, 3244–3248.

Chock, S. P., & Eisenberg, E. (1979) *J. Biol. Chem. 254*, 3229–3235.

Chock, S. P., Chock, P. B., & Eisenberg, E. (1979) *J. Biol. Chem. 254*, 3236–3243.

Dixon, M., & Webb, E. C. (1979) *Enzymes*, 3rd ed., pp 164–182, Longman Group, Ltd., London.

Douzou, P. (1977) *Cryobiochemistry*, Academic Press, London.

Douzou, P., Hui Bon Hoa, G., Maurel, P., & Travers, F. (1976) in *Handbook of Biochemistry and Molecular Biology* (Fasmann, G. D., Ed.) 3rd ed., Vol. I, pp 520–539, CRC Press, Cleveland, OH.

Engelborghs, Y., Marsh, A., & Gutfreund, H. (1975) *Biochem. J. 151*, 47–50.

Geeves, M. A., & Trentham, D. R. (1982) *Biochemistry 21*, 2782–2789.

Goldman, Y. E., Hibberd, M. G., Mc Cray, J. A., & Trentham, D. R. (1982) *Nature (London) 300*, 701–705.

Gutfreund, H. (1972) *Enzymes: Physical Principles*, Wiley-Interscience, London, New York, Sydney, and Toronto.

Gutfreund, H., & Trentham, D. R. (1975) in *Energy Transformation in Biological Systems*, Ciba Found. Symp. No. 31, pp 69–81, Associated Scientific Publishers, Amsterdam.

Highsmith, S., & Cook, R. (1983) in *Cell and Muscle Motility* (Dowben, R., & Shey, J., Eds.) Plenum Press, New York (in press).

Huennekens, F. M. (1963) in *Investigation of Rates and Mechanisms of Reactions* (Friess, S. L., Lewis, E. S., & Weissberger, A., Eds.) Vol. VIII, Part II, pp 1292–1312, Interscience Publishers, New York and London.

Huxley, H. E. (1969) *Science (Washington, D.C.) 164*, 1356–1367.

Jencks, W. P. (1969) *Catalysis in Chemistry and Enzymology*, McGraw-Hill, New York.

Johnson, K. A., & Taylor, E. W. (1978) *Biochemistry 17*, 3432–3442.
Keleti, T. (1983) *Biochem. J. 209*, 277–280.
Knack, I., & Röhm, K. H. (1981) *Hoppe-Seyler's Z. Physiol. Chem. 362*, 1119–1130.
Knowles, J. R. (1980) *Annu. Rev. Biochem. 49*, 877–919.
Kodama, T. (1981) *J. Biol. Chem. 256*, 2928–2933.
Kodama, T., & Woledge, R. C. (1979) *J. Biol. Chem. 254*, 6382–6386.
Krug, R. R., Hunter, W. G., & Grieger, R. A. (1976) *J. Phys. Chem. 80*, 2325–2341.
Kumamoto, J., Raison, J. K., & Lyons, J. M. (1971) *J. Theor. Biol. 31*, 47–51.
Laidler, K. J., & Peterman, B. F. (1979) *Methods Enzymol. 63A*, 234–257.
Levy, H. M., Sharon, N., & Koshland, D. E. (1959) *Proc. Natl. Acad. Sci. U.S.A. 45*, 785–791.
Londesborough, J. (1980) *Eur. J. Biochem. 105*, 211–215.
Lymn, R. W., & Taylor, E. W. (1971) *Biochemistry 10*, 4617–4624.
Malik, M. N., & Martonosi, A. (1972) *Arch. Biochem. Biophys. 152*, 243–257.
Margossian, S. S., & Lowey, S. (1978) *Biochemistry 17*, 5431–5439.
Marston, S. B. (1982) *Biochem. J. 203*, 453–460.
Massey, V., Curti, B., & Ganther, M. (1966) *J. Biol. Chem. 241*, 2347–2357.
Maurel, P. (1978) *J. Biol. Chem. 253*, 1677–1683.
Miyano, M. (1983) *Biochim. Biophys. Acta 743*, 207–211.
Mornet, D., Pantel, P., Audemard, E., & Kassab, R. (1979) *Biochem. Biophys. Res. Commun. 89*, 925–932.
Parenti-Castelli, G., Baracca, A., Fato, R., & Rabbi, A. (1983) *Biochem. Biophys. Res. Commun. 111*, 366–372.
Reimann, E. M., & Umfleet, R. A. (1978) *Biochim. Biophys. Acta 523*, 516–521.
Schaub, M. C., & Watterson, J. G. (1973) *FEBS Lett. 30*, 305–308.
Sivaramakrishnan, M., & Burke, M. (1982) *J. Biol. Chem. 257*, 1102–1105.
Sleep, J. A., Trybus, K. M., Johnson, K. A., & Taylor, E. W. (1981) *J. Muscle Res. Cell Motil. 2*, 373–399.
Taylor, E. W. (1979) *CRC Crit. Rev. Biochem. 6*, 102–164.
Taylor, R. S., & Weeds, A. G. (1977) *FEBS Lett. 75*, 55–60.
Tonomura, Y., & Inoue, A. (1975) in *MTP International Review of Science, Biochemistry Series I* (Racker, E., Ed.) Vol. 3, pp 121–161, Butterworths, London.
Travers, F., & Hillaire, D. (1979) *Eur. J. Biochem. 98*, 293–299.
Travers, F., & Barman, T. E. (1980) *Eur. J. Biochem. 110*, 405–412.
Travers, F., Bertrand, R., Roseau, G., & van Thoai, N. (1978) *Eur. J. Biochem. 88*, 523–528.
Travers, F., Barman, T. E., & Bertrand, R. (1979) *Eur. J. Biochem. 100*, 149–155.
Trentham, D. R. (1977) *Biochem. Soc. Trans. 5*, 5–22.
Trentham, D. R., Eccleston, J. F., & Bagshaw, C. R. (1976) *Q. Rev. Biophys. 9*, 217–281.
Wagner, R. D., & Weeds, A. G. (1977) *J. Mol. Biol. 109*, 455–473.
Weeds, A. G., & Taylor, R. S. (1975) *Nature (London) 257*, 54–56.
Wells, J. A., & Yount, G. (1982) *Methods Enzymol. 85B*, 93–116.
Wilkinson, K. D., & Rose, I. A. (1979) *J. Biol. Chem. 254*, 12567–12572.

Phospholipid Structure and the Packing of Cholesteryl Oleate at the Lipid/Water Interface†

Janice M. Smaby, Patricia C. Schmid, and Howard L. Brockman*

ABSTRACT: The miscibility and packing characteristics of cholesteryl oleate in films of phospholipids at the air/water interface were measured as a function of phospholipid structure. For phospholipids which differ only in the polar substituent on the phosphate, miscibility is positively correlated with the molecular areas of the pure phospholipids under comparable conditions. For choline phospholipids which differ in apolar substituents, miscibility is negatively correlated with the number of aliphatic groups and with the proportion of those groups containing cis unsaturation. Phospholipids containing saturated aliphatic moieties and lysophosphatidylcholines exhibited nonideal mixing in the monolayer phase. The miscibility data can be described by a geometric model in which cholesteryl esters are accommodated in the potential free area available in the apolar region of the surface phase. When applied at a surface pressure of 20 mN/m, it yields 18, 35, and 116 Å^2/molecule for the partial molecular areas of saturated chains, cis-unsaturated chains, and cholesteryl oleate, respectively. Thus, cholesteryl ester miscibility is regulated by phospholipid head group and aliphatic composition insofar as they determine the space available in the aliphatic region of the interface.

Long-chain esters of cholesterol are often perceived only as constituents of bulk lipid phases but do exhibit small solubilities in phospholipid bilayer membranes [e.g., see Janiak et al. (1974) and Gorrissen et al. (1980)] and in lipid films at the air/water interface. In the latter system, they are solubilized by a variety of non-cholesterol lipids (colipids) provided the acyl moiety of the cholesteryl ester contains cis unsaturation (Smaby et al., 1979). The position and extent of this unsaturation, the molar ratio of lipid components, and the packing density of the lipid components determine the distribution of cholesteryl ester between a bulk lipid phase and two immiscible

† From the Hormel Institute, The University of Minnesota, Austin, Minnesota 55912. *Received August 11, 1983.* This investigation was supported specifically by U.S. Public Health Service Research Grant HL 23003 from the National Heart, Lung and Blood Institute. General support was provided by Program Project Grant HL 08214 and by The Hormel Foundation. This work was done during the tenure of an Established Investigatorship (H.L.B.) of the American Heart Association with funds contributed in part by the Minnesota Affiliate.

0006-2960/84/0423-1955$01.50/0